

Electric carrier concentration in graphite: Dependence of electrical resistivity and magnetoresistance on defect concentration

A. Arndt, D. Spoddig, P. Esquinazi,* J. Barzola-Quiquia, S. Dusari, and T. Butz
Institut für Experimentelle Physik II, Universität Leipzig, Linnéstraße 5, D-04103 Leipzig, Germany

(Received 25 September 2009; published 2 November 2009)

We investigate the dependence of the electrical resistivity and magnetoresistance of single crystalline micrometer-sized graphite samples of a few tens of nanometers thick on the defect concentration produced by irradiation at low fluences. We show that the carrier density of graphite n is extremely sensitive to the induced defects for concentrations as low as ~ 0.1 ppm and follows $n \sim 1/R_V^2$ with R_V the distance between defects in the graphene plane. These and Shubnikov-de Haas oscillations results indicate that at least a relevant part of the carrier densities measured in graphite is not intrinsic.

DOI: [10.1103/PhysRevB.80.195402](https://doi.org/10.1103/PhysRevB.80.195402)

PACS number(s): 73.90.+f, 61.80.-x, 81.05.Uw

I. INTRODUCTION

The electronic properties of *ideal* graphite are actually not well known simply because *defect-free* graphite samples do not exist. In the last fifty years scientists flooded the literature with reports on different kinds of electronic measurements on graphite samples, providing evidence for carrier (electron plus hole) densities per graphene layer at low temperatures $n_0 \sim 10^{10} \dots 10^{12} \text{ cm}^{-2}$, see e.g., Refs. 1–3. However, in all those studies there is no knowledge whether the whole measured densities are intrinsic or influenced by lattice defects or impurities. Due to the special structure of ideal graphite this knowledge is relevant since one expects that its carrier density should be strongly dependent on lattice defects and impurities or adatoms.^{2,4} This expectation and taking into account that an exhaustive experience accumulated in gapless semiconductors—whose density of states should be similar to its counterpart in a semimetal—indicates so far that the measured n_0 is most probably due to impurities.⁵ A fundamental question remains unanswered, namely, how large is the intrinsic n_0 of ideal graphite?

Why is n_0 so important? Let us recapitulate some fundamental band-structure theoretical results for the graphite structure.² Two-dimensional (2D) calculations assuming a coupling γ_0 between nearest in-plane neighbors C atoms give a carrier density (per C atom) $n(T) = (0.3 \dots 0.4)(k_B T / \gamma_0)^2$ ($\gamma_0 \approx 3 \text{ eV}$ and T is the temperature). Introducing a coupling ($\gamma_1 \sim 0.3 \text{ eV}$) between C atoms of type α in adjacent planes one obtains $n(T) = a(\gamma_1 / \gamma_0^2)T + b(T / \gamma_0)^2 + c(T^3 / \gamma_0^2 \gamma_1) + \dots$ (a, b, c, \dots are numerical constants). In both cases $n(T \rightarrow 0) \rightarrow 0$. Neither in single layer graphene nor in graphite such T dependences were ever reported,⁶ i.e., a large density background n_0 was always measured and assumed as “intrinsic” without taking care of any influence from lattice defects (including edge effects⁷) or impurities. To fit experimental data and obtain a finite Fermi energy E_F , up to seven free parameters were introduced in the past, whereas in the simplest case $E_F \propto \gamma_2$.^{2,8}

Clearly, any evidence that speaks against an intrinsic origin of—even a part of—the measured n_0 in graphite samples would cast doubts on the relevance of related electronic band-structure parameters obtained in the past and will help significantly to clarify observed transport phenomena. As in the case of gapless semiconductors⁵ this requires a formi-

dable experimental task. For example, to prove that the measured $n_0 = 2 \times 10^8 \text{ cm}^{-2}$ in Ref. 9 is due to vacancies/interstitials requires a vacancy resolution better than 0.05 ppm. Although nowadays the concentration of impurities in graphite can be measured with ~ 0.1 ppm resolution, there is no experimental method that allows us to determine with such a precision the number of vacancies or C interstitials. In spite of that and because of these difficulties we would like to start the discussion on the origin of n_0 , postulating that at least part of it cannot be intrinsic.

In this study we measured the change in the electrical resistance of thin crystalline graphite samples as a function of defect concentrations between ~ 0.1 to $\sim 10^3$ ppm. We measured a decrease in the resistance at the lowest induced defect concentration due to—as theoretically expected—an increase in the carrier density. Because the induced defect concentration is at least two orders of magnitude *smaller* than the usual impurity concentration of high-purity graphite samples, without taking into account the (unknown) density of vacancies and interstitials every sample has, one should doubt on the origin of the measured density of carriers. Since these resistance measurements are done at room temperature for reasons that are clarified below, measurements of the Shubnikov-de Haas (SdH) oscillations were done at 4K before and after inducing a defined defect density in a thin graphite sample and also for the corresponding bulk sample. The results from these measurements strengthen the main message of these studies, indicating that a relevant part of the carrier densities measured in graphite is not intrinsic.

The studies presented in this work provide answers to the following basic questions:

(1) Can a single vacancy/interstitial provide \sim one carrier into the conduction band even if they are several hundreds of nm apart (ppm concentration)? This is a relevant issue specially because we expect that the Fermi wavelength in graphite $\lambda_F \approx 1 \text{ } \mu\text{m}$.¹⁰

(2) Can the resistivity of graphite change with such small defect concentrations?

(3) How reliable are band-structure parameters of graphite obtained from the field-induced quantum oscillations in the resistivity (or magnetization)?

(4) Why there is an apparent maximum value for n_0 of several times 10^{12} carriers per cm^2 in graphite samples?

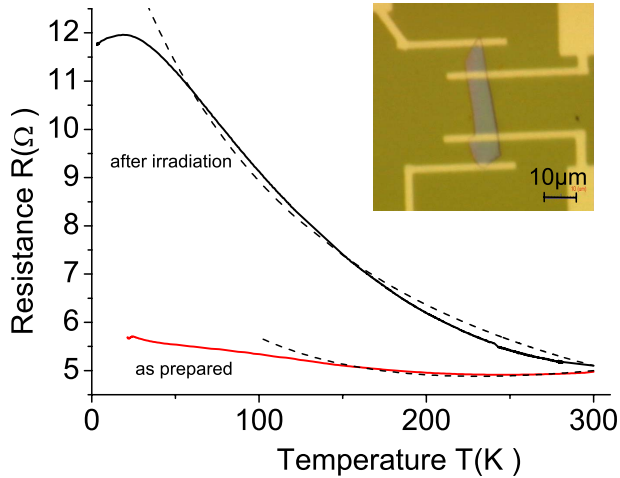


FIG. 1. (Color online) Temperature dependence of the resistance of sample 3 in the as-prepared state and after proton irradiation with a fluence of $9 \times 10^{13} \text{ cm}^{-2}$ (continuous lines). Note the large change in $R(T)$ after inducing only ~ 3 ppm vacancy density. The dashed lines are obtained assuming a Fermi energy $E_F = E_0 + k_B T$ and a T^{-2} dependence for the mean-free path, see text for details. The inset shows an optical microscope picture of sample 1 with gold electrodes on top.

II. EXPERIMENTAL DETAILS

We irradiated three ~ 60 nm thick and tens square micrometer samples under ambient conditions with a focused proton microbeam of 2.25 MeV energy scanned over the samples. A photo of sample 1 can be seen in Fig. 1. Particle-induced x-ray emission measurements were done *in situ* and revealed a total concentration of $\sim 20 \mu\text{g/g}$ of nonmagnetic impurities except hydrogen of concentration $0.5 \pm 0.3\%$.¹¹ The magnetoresistance of a fourth sample of size $11 \times 2 \times 0.015 \mu\text{m}^3$ was measured at three different parts, each of length $\approx 1.6 \mu\text{m}$ and irradiated with 30 keV Ga^+ ions. In this sample SdH oscillations were measured at 4K before and after irradiation and also for the corresponding bulk sample.

The graphite flakes were obtained by exfoliation of a highly oriented pyrolytic graphite (HOPG) sample ZYA grade and using ultrasonic technique. We obtained several flakes that we selected them using microscopic and Raman techniques. This precharacterization of the selected single crystalline regions is done with a dual-beam electron microscope and micro-Raman. Micro-Raman measurements show the absence of disordered peak, indicating a highly ordered structure. Those regions of typical size $< 20 \times 5 \mu\text{m}^2$ and less than 100 nm thickness are observable by electron back scattering diffraction and transmission electron microscopy (see for example the studies done in Refs. 9 and 12). The crystallographic orientation is always with the main area parallel to the graphene layers.

The samples were fixed on Si substrates, which have an insulating 300 nm thick Si_3N_4 layer. These substrates were fixed with silver paste on a chip carrier. This carrier was fixed in a special irradiation chamber that allows resistance measurements *in situ* as a function of fluence and time during and after irradiation. The resistance measurements were

done using an ac bridge (Linear Research LR700) with a relative resolution better than 10^{-5} . The temperature was monitored with a Pt thermometer fixed on the sample holder. The measured temperature remained stable within 0.05 K through the whole irradiation and ~ 5 h after.

The samples' contacts were prepared by electron-beam lithography. The covering of the samples with the photoresist protected them from electron-irradiation damages the scanning electron microscope produce, see e.g., Ref. 13. A bottom layer of Pt and a top layer of Au were deposited by thermal evaporation and served as contacts, see Fig. 1. The in-plane resistivity of the measured samples was $\rho \approx 65 \pm 10 \mu\Omega \text{ cm}$ at 300 K. This value agrees with those obtained in previous studies.¹²

III. RESULTS AND DISCUSSION

A. Changes in the electrical resistance vs defect concentration

Figure 2(a) shows the relative change in the resistance vs time during and after irradiation of sample 3 at 297 K. The curves are obtained at different initial relaxed states after application of a certain proton fluence. When the beam starts to hit the sample we observe a clear decrease in the resistance, whose amount depends on the fluence used and on the initial sample state. Figure 2(b) shows the resistance change relative to the sample virgin state. In this figure $t=0$ s means the time at which the beam stops irradiating the sample. Remarkable is that for all samples in the virgin state we observe a *decrease* in the resistance of a few percent for induced defect density < 3 ppm (average defect distance $R_V > 100$ nm) that remains after several hours after irradiation, i.e., in the relaxed state $R(t \geq 1 \text{ h})$, see curves (1–3) in Fig. 2(b). In Fig. 3 we show this relative change for samples 2 and 3. A further increase in the fluence increases the resistance in the relaxed state, see Fig. 3. The explanation for this behavior is that defects increase the carrier density n , as theoretically suggested.⁴ But because defects also act as scattering centers, both the carrier mean-free path $l(R_V)$ and $n(R_V)$ have to be taken into account.

We assume graphite as a structure composed of weakly coupled graphene sheets.¹⁴ Within a factor of two the initial value at 297 K before irradiation for the carrier density is $n_i \sim 6 \times 10^{10} \text{ cm}^{-2}$ and for the mean-free path $l_i \sim 50 \text{ nm}$.⁹ The smallness of l at 297 K in comparison to the sample size allows us to use the Boltzmann-Drude semiclassical approach. This is important because for our sample sizes and at $T \leq 150$ K there is no straightforward theoretical approach that includes ballistic and diffusive scattering that allows us to obtain in a simple way $n(R_V)$ from the resistance. Hall-effect measurements are not necessarily preferred to obtain $n(R_V)$ since (i) the Hall signal depends on at least six unknown parameters (n, l, m^* for electrons and holes independently) that change with defect concentration and T ; (ii) conventional multiband approaches appear to be inadequate for graphite,⁹ and (iii) added to these difficulties, the Hall signal of graphite can be anomalous at $T < 150$ K.¹⁵

Following the stopping and range of ions in matter (SRIM) simulations¹⁶ the produced defect concentration at a proton fluence of 10^{13} cm^{-2} would be $n_V \sim 10^9 \text{ cm}^{-2}$. As-

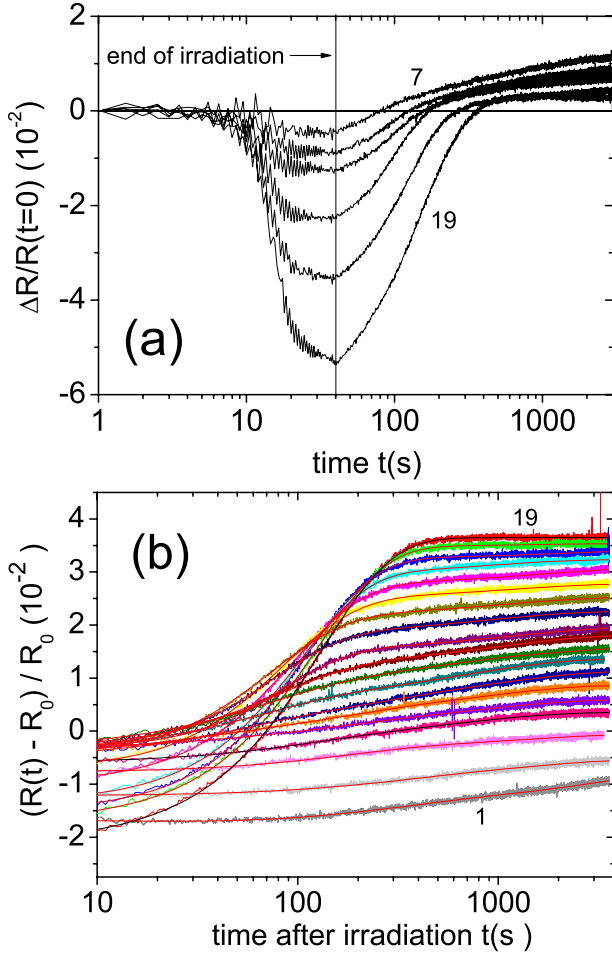


FIG. 2. (Color online) (a) Relative change in the resistance $R(t) - R(0)/R(0)$ measured vs time during and after the proton beam hits sample 3. The different curves were obtained at different starting relaxed conditions after irradiation of $3.1, 4.0, 4.3, 6.4, 7.2, 9.0 \times 10^{13}$ protons per cm^{-2} , corresponding to the curve numbers 7, 9, 10, 14, 16, 19, from top to bottom. The small oscillations in the resistance observed during irradiation are an artifact due to the overlapping of the proton current and the ac current of the resistance bridge. (b) Change in resistance relative to its value in the virgin state R_0 vs time. The time scale is taken from the time at which the beam does not hit the sample anymore, i.e., the minimum in $\Delta R/R(0)$ in (a). Note the decrease in resistance with irradiation for the first three curves (1–3 from bottom) even in the relaxed states (after 1 h). As in (a) the different curves are taken from the sample at different initial states irradiated with fluences $(1, 2, \dots, 19) = (1, 1.5, 2.0, \dots, 9) \times 10^{13}$ protons/ cm^{-2} .

suming that each defect in the graphene plane increases by one the carrier number, the increase in carrier density after irradiating such fluence will be $n_V \sim 10^{-2} n_i$, or in terms of the related wave vector $k_V \approx (\pi n_V)^{1/2} = 5.6 \times 10^4 \text{ cm}^{-1} \approx 0.1 k_F$. This simple estimate reveals that such small defect concentrations are relevant for the transport.

At 297 K the produced defects by irradiation are metastable, see Fig. 2. Therefore, we plot in Fig. 3 the relative change in the resistance just at the end of the irradiation R_{\min} with respect to the virgin state R_0 , i.e., $R_{\min}/R_0 - 1$ (close and open circles in Fig. 3). Another possibility is to plot the

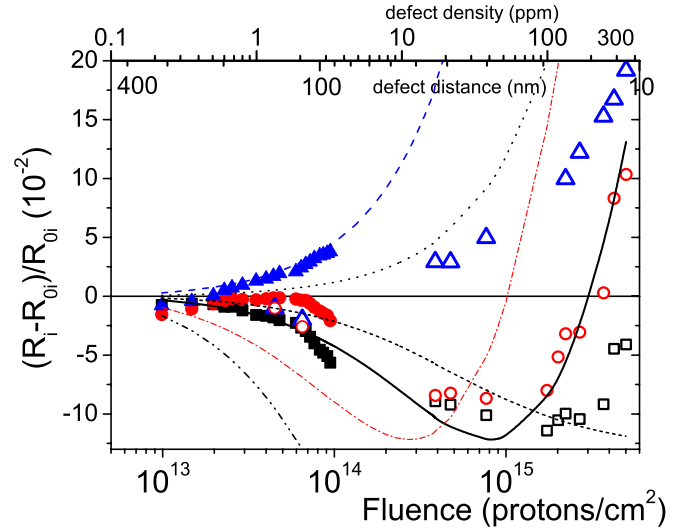


FIG. 3. (Color online) Relative change in resistance vs fluence for sample 2 (open symbols) and sample 3 (close symbols). The upper x axis shows the corresponding scales as average defect distance within a graphene plane R_V and the defect density in parts per million (ppm). The triangles represent the change in the resistance in the relaxed state after irradiation relative to the virgin state R_0 , i.e., $R(t \geq 1 \text{ h})/R_0 - 1$. The circles are obtained from $R_{\min}/R_0 - 1$ and the squares $R_{\min}/R(t \geq 1 \text{ h}) - 1$. The curves were obtained from Eq. (1) with the following parameters: $n_V = 0.1/R_V^2$, $l_i = 50 \text{ nm}$ (long dashed); $0.1/R_V^2$, 20 nm (dot); $1/R_V^2$, 50 nm (continuous); $3/R_V^2$, 150 nm (red dash-dot); $3/R_V^2$, 50 nm (dash-double dot). The short-dash curve was obtained assuming the usual 3D relation $R \propto 1/\ln$ and with $n_V = 0.9/R_V^2$, $l_i = 150 \text{ nm}$. Note that with this 3D relationship no minimum in the measured range is obtained within a broad variation in parameters.

relative change with respect to the resistance taken one hour after irradiation R_{rel} , i.e., $R_{\min}/R_{rel} - 1$ (close and open squares in Fig. 3). Both ways minimize the influence of annealing effects and provide a similar behavior. These relative changes indicate that the resistance reaches a minimum $\sim 90\%$ of its initial value at $R_V = 20 \dots 30 \text{ nm}$, see Fig. 3. At higher fluences the resistance increases because the decrease in l starts to overwhelm the increase in n .

A quantitative description of these data can be done taking into account the two-dimensional resistivity¹⁷ $\rho = 2/e^2 v_F^2 N(E_F) \tau_F$, where v_F , E_F , τ_F are the Fermi velocity, the Fermi energy, and the scattering relaxation time at Fermi energy. Using $N(E_F)$ for clean graphene,⁴ the expression for $E_F = \hbar v_F k_F$ and $\tau_F = l/v_F$, one arrives at the simple expression $\rho = (\pi/2)^{1/2} (\hbar/e^2) l^{-1} n^{-1/2}$. Furthermore, the carrier density increases as $n = n_i + n_V$, where $n_V = 1/R_V^2$ for one carrier per defect. Following Mathiessen's rule, the mean-free path is given by $l^{-1} = l_i^{-1} + l_V^{-1}$, where l_i is the initial value due to all scattering centers before irradiation and l_V is the mean-free path due to the produced defects. The relative change in resistance can be written as

$$\frac{R - R_0}{R_0} = \left(\frac{1}{1 + (n_V/n_i)} \right)^{1/2} \left(1 + \frac{l_i}{l_V} \right) - 1. \quad (1)$$

The solid curve shown in Fig. 3 is obtained with $l_V = 1.15 \times 10^6 [\text{cm}^{-1}] R_V^2 [\text{cm}^2]$ for $l_i = 50 \text{ nm}$ and $n_V = 1/R_V^2$. Within

logarithmic corrections, the obtained $l_V(R_V)$ function agrees quantitatively with that found in Ref. 4. In Fig. 3 we show also other curves obtained using other values for l_0 and prefactors for $n_V(R_V)$ as well as assuming the usual three-dimensional (3D) relationship $R \propto 1/n$ instead of $1/n^{1/2}$. The comparison indicates that within a factor of two n_V is indeed given by $1/R_V^2$ (for $R_V > 10$ nm) and that the usual 3D relationship for R cannot describe the observed behavior within a reasonable range of parameters.

The remarkable decrease with temperature of the resistance as well as the observed change in the temperature dependence of graphite after inducing only ~ 3 ppm defect density ($R_V \sim 100$ nm) is mainly given by the decrease in $E_F \approx E_F(0) + k_B T \propto \sqrt{n(T)}$ with temperature. As shown in Ref. 9 E_F is basically determined by thermal electrons (note that $E_F \sim 330$ K for $n = 6 \times 10^{10}$ cm $^{-2}$) and its T dependence overwhelms that of $l(T)$. With $E_F(T)$, $l_i(T) \propto T^{-2}$ (Ref. 9) and the parameters obtained from Fig. 3 in Eq. (1), one can understand the observed temperature dependence of the resistance above ~ 100 K, see Fig. 1. We stress that at lower temperature the Boltzmann-Drude approach loses its validity.

A quantitative description of the observed time dependence (Fig. 2) shows that this is governed by interstitial migration processes¹⁸ and single vacancy diffusion¹⁹ with activation energies ~ 0.87 eV and ~ 0.93 eV, respectively. The migration processes annihilate partially the produced defects and at fluences $\geq 2 \times 10^{13}$ cm $^{-2}$ (for sample 3) the relaxed resistance increases, indicating that the graphite structure remains with a certain amount of defects decreasing the overall carrier mobility.

Defect-induced magnetic order in graphite is a subject of actual research. Ion irradiation is one of the methods to study systematically the effects of defects on the magnetism, see, e.g., Ref. 20 and references therein. It has been recently found that proton irradiation of HOPG at 110 K triggers a larger ferromagnetic signal in comparison with similar irradiations done at room temperature.²¹ The results presented in this study show a considerable relaxation of defects at room temperature, just after a few hours after irradiation. This defect relaxation provides a possible explanation for the smaller ferromagnetic signals observed in irradiated graphite at 300 K.

B. Changes in the magnetoresistance with defects

The band parameters of graphite were obtained in the past mostly on macroscopic samples and usually from magneto-optical studies, SdH and de Haas-van Alphen oscillations, cyclotron resonance, etc. Because in usual graphite samples the defect density is neither negligible nor can be expected to be homogeneous, the defect-dependent carrier density should be neither small nor homogeneously distributed. Within the 11 μ m length of sample 4 we measured the magnetoresistance at 4 K at different parts of the sample of similar area and calculate its first derivative. The SdH oscillations depend on the sample position, see Fig. 4, indicating clearly inhomogeneities in the carrier concentration within micrometers in agreement with electric field microscopy (EFM) results

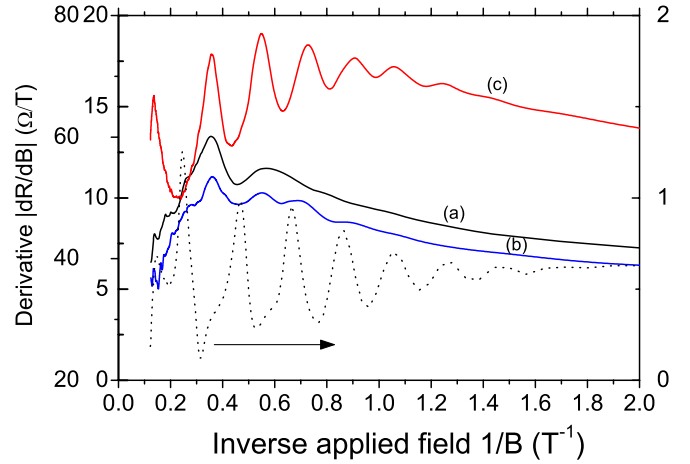


FIG. 4. (Color online) First derivative of the magnetoresistance measured at 4 K in two parts (a) and (b) of similar area $2 \times 1.6 \mu\text{m}^2$ separated by $3 \mu\text{m}$ in sample 4 ($0-20 \Omega/\text{T}$ range). (c) Sample part (a) after irradiation with a fluence of 5×10^{11} Ga $^{+}$ -ions per cm 2 ($20-80 \Omega/\text{T}$ range). The dashed curve was obtained for the bulk sample of size $2 \times 1 \times 0.2 \text{ mm}^3$ at 4 K. The magnetic field was applied normal to the graphite layers.

that revealed submicrometer domainlike carrier density distributions in graphite surfaces.²²

For the measured sample area that gives curve (a) in Fig. 4 and within experimental resolution, there are no SdH oscillations up to a field $B \approx 1.8$ T in clear contrast to the bulk sample, see Fig. 4. This fact can be understood assuming that in most of this sample part $n_0 \leq 10^9$ cm $^{-2}$. Then, the corresponding Fermi wavelength $\lambda_F \geq 0.8 \mu\text{m}$ is of the order of the sample size and larger than the cyclotron radius $r_c = m^* v_F / eB$ for $B > 0.07$ T assuming $m^* = 0.01m$ (m is the free-electron mass). In this case we do not expect to observe any SdH oscillations. However, for $B \approx 1.8$ T and 2.8 T two maxima are observed. From the measured “period” P in $1/B$ as well as from the first field at which the first maximum appears we estimate the existence of domains of size $< 2r_c \leq 100$ nm in which $\lambda_F \leq 50$ nm, i.e., domains with $n_0 \geq 10^{11}$ cm $^{-2}$ within a matrix of much lower carrier concentration. This indicates that the description of the SdH oscillations in real graphite samples can be achieved only within the framework of inhomogeneous 2D systems,^{23,24} an issue that to the best of our knowledge was neither applied nor discussed for graphite in the past.

The selected Ga $^{+}$ irradiation produced an average defect concentration of $\sim 10^{12}$ cm $^{-2}$, i.e., $\sim 10^3$ ppm (Ga implantation ≤ 1 ppm) in the thin graphite sample, “homogenizing” its carrier density distribution. After irradiation the SdH oscillations are clearly observed for $B \geq 0.7$ T, see Fig. 4. Their period $0.16 \text{ T}^{-1} \leq P \leq 0.23 \text{ T}^{-1}$ is within the range found in literature^{2,25} and indicates $n_0 \sim 3 \times 10^{11}$ cm $^{-2}$.

Finally, if a relevant part of the reported carrier concentration in graphite is due to defects, why does it appear to saturate at values of several times 10^{12} carriers per cm 2 ($\geq 3 \times 10^{-4}$ carriers per C atom)? We note that such saturation is observed in gapless semiconductors with increasing donor concentration.⁵ Therefore, we might also expect it when the average distance between defects is of the order of

the range of modification of the electronic structure produced by, e.g., a single vacancy. This was found experimentally to be ~ 3 nm,²⁶ implying that the defect-induced carrier density n_0 cannot be larger than $\sim 10^{13}$ cm⁻².

IV. CONCLUSIONS

Concluding, the obtained results indicate that a concentration of defects (or impurities) of ~ 0.2 ppm can generate a carrier density $\sim 10^9$ cm⁻² affecting the transport properties. This is an extraordinary sensitivity to defects. Taking into account that, in best case, we have an impurity concentration ≤ 20 ppm, except for hydrogen $\leq 1\%$, plus an unknown concentration of vacancies and interstitials, we should doubt about the assumed “intrinsic” origin of the measured carrier

concentrations in graphite. The behavior of SdH oscillations in micrometer-sized graphite regions and their changes after introducing defects support the above statement and indicate that real graphite is composed by an inhomogeneous distribution of carrier density, in agreement with electric-force microscopy measurements done in the past on similar oriented graphite samples.

ACKNOWLEDGMENTS

This work has been possible with the support of the DFG under Grant No. DFG ES 86/16-1. S.D. is supported by Leipzig School of Natural Sciences (BuildMona). One of the authors (P.E.) gratefully acknowledges correspondence with A. V. Krasheninnikov and F. Guinea.

*esquin@physik.uni-leipzig.de

- ¹J. W. McClure, IBM J. Res. Dev. **8**, 255 (1964).
- ²B. T. Kelly, *Physics of Graphite* (Applied Science Publishers, London, 1981).
- ³A. Grüneis *et al.*, Phys. Rev. Lett. **100**, 037601 (2008).
- ⁴T. Stauber, N. M. R. Peres, and F. Guinea, Phys. Rev. B **76**, 205423 (2007).
- ⁵I. M. Tsidilkovski, *Electron Spectrum of Gapless Semiconductors*, Springer Series in Solid-State Sciences Vol. 116 (Springer, New York, 1997).
- ⁶Note, however, that the data obtained in Ref. 9 indicate $n[\text{cm}^{-2}] \sim n_0 + 7 \times 10^5 T^2$ (within factor of two), or $n = n_0 + 10^5 T^2 + 7.5 \times 10^3 T^3$ with T in K.
- ⁷Y. Kobayashi, K.-I. Fukui, T. Enoki, and K. Kusakabe, Phys. Rev. B **73**, 125415 (2006).
- ⁸R. O. Dillon, I. L. Spain, and J. W. McClure, J. Phys. Chem. Solids **38**, 635 (1977).
- ⁹N. García, P. Esquinazi, J. Barzola-Quiquia, B. Ming, and D. Spoddig, Phys. Rev. B **78**, 035413 (2008).
- ¹⁰J. C. González, M. Muñoz, N. García, J. Barzola-Quiquia, D. Spoddig, K. Schindler, and P. Esquinazi, Phys. Rev. Lett. **99**, 216601 (2007).
- ¹¹W. Anwand, G. Brauer, D. Grambole, A. Setzer, and P. Esquinazi (unpublished).
- ¹²J. Barzola-Quiquia, J.-L. Yao, P. Rödiger, K. Schindler, and P. Esquinazi, Phys. Status Solidi A **205**, 2924 (2008).
- ¹³D. Teweldebrhan and A. A. Balandin, Appl. Phys. Lett. **94**, 013101 (2009).
- ¹⁴Y. Kopelevich and P. Esquinazi, Adv. Mater. (Weinheim, Ger.) **19**, 4559 (2007).
- ¹⁵Y. Kopelevich, J. C. M. Pantoja, R. R. da Silva, F. Mrowka, and P. Esquinazi, Phys. Lett. A **355**, 233 (2006).
- ¹⁶J. F. Ziegler, *The Stopping and Range of Ions in Matter* (Pergamon Press, New York, 1977).
- ¹⁷K. Nomura and A. H. MacDonald, Phys. Rev. Lett. **96**, 256602 (2006).
- ¹⁸K. Niwase, Phys. Rev. B **52**, 15785 (1995).
- ¹⁹G.-D. Lee, C. Z. Wang, E. Yoon, N.-M. Hwang, D.-Y. Kim, and K. M. Ho, Phys. Rev. Lett. **95**, 205501 (2005).
- ²⁰P. Esquinazi, J. Barzola-Quiquia, D. Spemann, M. Rothermel, H. Ohldag, N. García, A. Setzer, and T. Butz, J. Magn. Magn. Mater. (to be published).
- ²¹J. Barzola-Quiquia, P. Esquinazi, M. Rothermel, D. Spemann, T. Butz, and N. García, Phys. Rev. B **76**, 161403(R) (2007).
- ²²Y. Lu, M. Muñoz, C. S. Steplecaru, C. Hao, M. Bai, N. García, K. Schindler, and P. Esquinazi, Phys. Rev. Lett. **97**, 076805 (2006); See also the comment by S. Sadewasser and Th. Glatzel, *ibid.* **98**, 269701 (2007) and the reply by Y. Lu *et al.*, *ibid.* **98**, 269702 (2007); R. Proksch, Appl. Phys. Lett. **89**, 113121 (2006).
- ²³V. T. Dolgoplov, A. A. Shashkin, G. V. Kravchenko, I. M. Mukhametzhano, M. Wendel, J. P. Kotthaus, L. W. Molenkamp, and C. T. Foxon, JETP Lett. **63**, 63 (1996).
- ²⁴N. Harrison and J. Singleton, J. Phys.: Condens. Matter **13**, L463 (2001).
- ²⁵I. A. Luk'yanchuk and Y. Kopelevich, Phys. Rev. Lett. **93**, 166402 (2004).
- ²⁶P. Ruffieux, O. Gröning, P. Schwaller, L. Schlapbach, and P. Gröning, Phys. Rev. Lett. **84**, 4910 (2000).